



## Automated docking of 82 *N*-benzylpiperidine derivatives to mouse acetylcholinesterase and comparative molecular field analysis with 'natural' alignment

Philippe Bernard<sup>a</sup>, Dmitri B. Kireev<sup>a</sup>, Jacques R. Chrétien<sup>a,\*</sup>, Pierre-Louis Fortier<sup>b</sup> & Lucien Coppet<sup>b</sup>

<sup>a</sup>Laboratoire de Chimiométrie, Université d'Orléans, BP 6759, F-45067 Orléans Cedex 2, France; <sup>b</sup>Centre d'Etude du Bouchet, D.G.A., B.P. No. 3, F-91710 Vert le Petit, France

Received 20 January 1998; Accepted 18 June 1998

**Key words:** reversible AChE inhibitors, systematic search, 3D QSAR

### Summary

Automated docking and three-dimensional Quantitative Structure-Activity Relationship studies (3D QSAR) were performed for a series of 82 reversible, competitive and selective acetylcholinesterase (AChE) inhibitors. The suggested automated docking technique, making use of constraints taken from experimental crystallographic data, allowed to dock all the 82 substituted *N*-benzylpiperidines to the crystal structure of mouse AChE, because of short computational times. A 3D QSAR model was then established using the CoMFA method. In contrast to conventional CoMFA studies, the compounds were not fitted to a reference molecule but taken in their 'natural' alignment obtained by the docking study. The established and validated CoMFA model was then applied to another series of 29 *N*-benzylpiperidine derivatives whose AChE inhibitory activity data were measured under different experimental conditions. A good correlation between predicted and experimental activity data shows that the model can be extended to AChE inhibitory activity data measured on another acetylcholinesterase and/or at different incubation times and pH level.

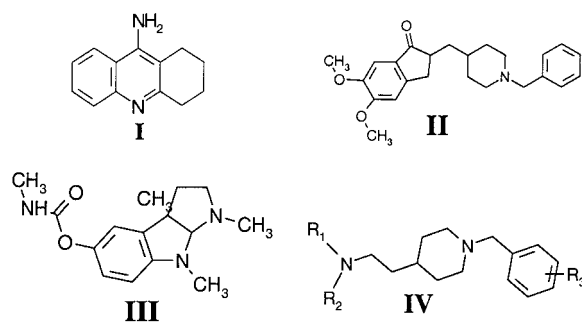
### Introduction

Alzheimer's disease (AD) is a progressive neurodegenerative disease affecting an increasingly important part of the elderly population. This pathology manifests itself clinically by a memory loss and biochemically by the deregulation of neurotransmission, e.g. serotonergic, dopaminergic and cholinergic systems [1]. The memory deficit in the patients afflicted by AD apparently correlates with the alteration of the basal forebrain cholinergic neurons [2]. Biochemical experiments have evidenced the crucial importance of decreasing cholinergic activity in AD patients [3]. Currently, searching for a chemotherapy of the memory loss attributed to AD is focused on this cholinergic hypothesis [4].

The cholinergic hypothesis has initiated clinical studies [5] testing the efficiency of AChE inhibitors in alleviating the disease symptoms. It has been shown that some AChE inhibitors are able to treat memory problems in AD patients. AChE inhibitors increase the ACh level and produce a significant benefit in the AD reversion [6]. The importance of research on AChE inhibitors is emphasized by the fact that two approved drugs for the treatment of AD are AChE inhibitors, (i) 1,2,3,4-tetrahydro-9-aminoacridine (Tacrine or Cognex), **I** and (ii) *N*-benzylpiperidine (E-2020, Aricept) **II** [7]. Some other AChE inhibitors, such as physostigmine **III**, galanthamine and huperazine A, are being clinically tested [8].

The current priority is to propose novel AChE inhibitors having less side effects, e.g. liver toxicity, and permitting to increase the ACh concentration in the

\*To whom correspondence should be addressed.



Scheme 1. Structures I–IV.

cholinergic neurones. However, further optimization of the therapeutic properties for the AChE inhibitors requires (i) better understanding of the mechanism of inhibitor-protein interaction, and (ii) finding a tool to predict the activity of new molecules. Approaches related to computational chemistry may help to resolve these two problems.

Among various AChE inhibitors, a series of 82 *N*-benzylpiperidine derivatives [9, 10] **IV** was chosen for the present study. These compounds are competitive, reversible, potent and selective inhibitors of acetylcholinesterase. A combination of a high AChE inhibitory activity with a low toxicity level makes them appropriate candidates for application to the treatment of AD.

Previous computational studies [11–17], focusing on this class of AChE inhibitors, can be clearly subdivided into two groups according to the computational methods used: (i) the receptor based studies, which deal with the modelling of ligand-receptor interactions through docking [11–13] or molecular dynamics (MD) [14], and (ii) quantitative structure-activity relationships (QSAR) analyses [15–17], which do not need an *a priori* hypothesis about the receptor structure.

Docking or MD studies [11–14] are computationally expensive and, therefore, they were applied only to small series numbering from 1 to 7 molecules. While, in general, receptor-based techniques provide accurate geometries of ligand-receptor complexes, they cannot be used for predictions of binding affinity or inhibitory activity, because of accumulated imprecisions from the multiple calculations of the ligand-receptor interaction energy, which are necessary to evaluate the free energy of the ligand-receptor complex. The applicability of the receptor-based methods to the drug design problems was recently reviewed by Kuntz et al. [18].

QSAR studies on reversible AChE inhibitors [15–17] were performed using either Comparative Molecular Field Analysis (CoMFA) [19] or conventional 2D QSAR methods. The former method, CoMFA, needs the studied molecules to be aligned in the three dimensional (3D) space. In conventional CoMFA studies, as in the first study by Cramer et al. [19], the molecules are fitted to a reference molecule. This reference molecule should be the most rigid of the active molecules. In this case, the molecule is always in its ‘biologically active’ conformation. However, in the case when active molecules are flexible, finding an appropriate alignment becomes a complicated task with high probability of a misleading result.

In case of known receptor structure, applying receptor-based methods can remove all ambiguity when choosing an alignment for flexible molecules. An ideal solution would be to dock all available molecules to the receptor, this would create an incontestable ‘natural’ alignment for the CoMFA model. In practice, however, this may prove a time consuming procedure. Moreover, in many cases, it would not completely remove the ambiguity related to the choice of the ‘biologically active’ conformation, because of the possibility of multiple hypotheses for the structure of the ligand-receptor complex. A reasonable and economic intermediate solution for the problem was suggested by Cho et al. [16] and Waller et al. [20] who used alignment rules based on experimentally determined structural constraints. Below in the present paper, we shall show, however, that this approach does not always produce a pertinent result.

This paper describes a special case in which, due to a ‘critical’ mass of available experimental data, it has become possible to dock all 82 benzylpiperidine AChE inhibitors to the catalytic site of the mouse AChE in an unequivocal manner and with reasonable computational expenses. The docked inhibitor

structures were then used as a 'natural' alignment to feed CoMFA. This paper aims to show that this total docking was indispensable to obtain a high quality CoMFA model. While being defined as 'special', such a case of the synergistic cooperation of receptor-based and QSAR techniques may become, however, more and more common due to rapidly growing libraries of available 3D protein structures and their complexes with biologically active ligands. In such cases, following our methodology would allow to rapidly create robust 'natural' alignments and to exploit them as input to 3D QSAR methods.

## Methods

### *Automated docking*

**Enzyme.** The crystal AChE structures were obtained from the Brookhaven Protein Data Bank (PDB). Two AChE proteins are presently available from PDB: one from *Torpedo californica* (TAcHE) (PDB code: 1ACE) and the other from mouse (MAChE) (PDB code: 1MAH). Since the inhibitory activity data used in the present study were measured on the MAChE it was preferable to perform our docking study on this enzyme. To make the structure suitable for further modeling, hydrogen atoms were added to the original PDB structure using the BIOPOLYMER module of Sybyl [21]. Then the geometry of the protein was optimized using the AMBER force field [22].

Further intention was to exploit known crystal structures of ligand-enzyme complexes as a source of geometric constraints for the automated docking procedure. However, it was not directly possible as crystallized ligand-enzyme complexes are only available for TAcHE. The structures of the complexes of TAcHE with decamethonium, edrophonium or THA were recently reported [23]. Two of the three inhibitors, decamethonium and edrophonium, possess a quaternary nitrogen bound to the 'catalytic anionic site' by a  $\pi$ -cation interaction with Trp84 [24]. The working hypothesis of this study was to consider that the quaternary piperidinic nitrogen of *N*-benzylpiperidine binds to the same site. Hence, the position of this atom was used as an anchor.

The next step was to project the quaternary nitrogen from TAcHE onto MAChE. Some of the residues belonging to peripheral and catalytic sites were used to align two protein structures by means of the Sybyl ANALYSE/FIT ATOMS option. In Figures 1a, b

some residues of the peripheral and catalytic sites and the position of the inhibitor's quaternary nitrogen are shown in both TAcHE and MAChE.

However, before accepting the above hypothesis we also checked another reasonable one. Indeed, Pang and Kozikowski [11], studying the binding mode of E2020 **II**, suggested, along with two other complex structures, a complex of this inhibitor with the catalytic cleft of TAcHE, in which the ammonium group interacts with Trp279. To verify this second hypothesis, we used an active inhibitor from our series, compound **25**. The coordinates of the anchor point were taken the same as the coordinates of the ammonium group of decametonium interacting with Trp279 of TAcHE (in MAChE this residue corresponds to Trp286). The docking of compound **25** did not give solutions with the inhibitor inside the catalytic cleft; the inhibitor was pushed outside the protein. This result is not surprising as compound **25** is much more bulky than E-2020.

A homology study was made between the two acetylcholinesterases considered in order to verify the necessity of using the MAChE structure rather than the TAcHE one currently used in most modelling studies [11–14]. Our intention was to find out whether using MAChE instead of TAcHE is justified. First, it was found that the primary structures of these two enzymes are rather different. This difference is due to omissions and 'mutations' of more than 10% of the residues in TAcHE compared to MAChE. Some of these differing fragments are located close to the peripheric and catalytic sites and may interact with inhibitors. The most pertinent example is the replacement of Phe330 in TAcHE by Tyr337 in MAChE. Tyr337 belongs to a hydrophobic domain {Phe295, Phe297, Tyr337, Phe338, Tyr341} which interacts with some of the benzylpiperidine derivatives. This evidence suggests that the same inhibitor may have different affinities to these two acetylcholinesterases and, therefore, using the MAChE structure is justified.

On the other hand, the 3D structure with the catalytic and peripheric sites including Ser203, Trp286, Trp86, Tyr124 is conserved in both proteins. It allows a reliable alignment of their 3D structures using these four residues as a reference in the FIT\_ATOMS procedure of Sybyl.

**Ligands.** Each of the 82 ligands was modeled using Sybyl 6.3 on a Silicon Graphics INDY R5000 station. The starting conformations were optimized by molecular mechanics algorithm using the Tripos Force Field

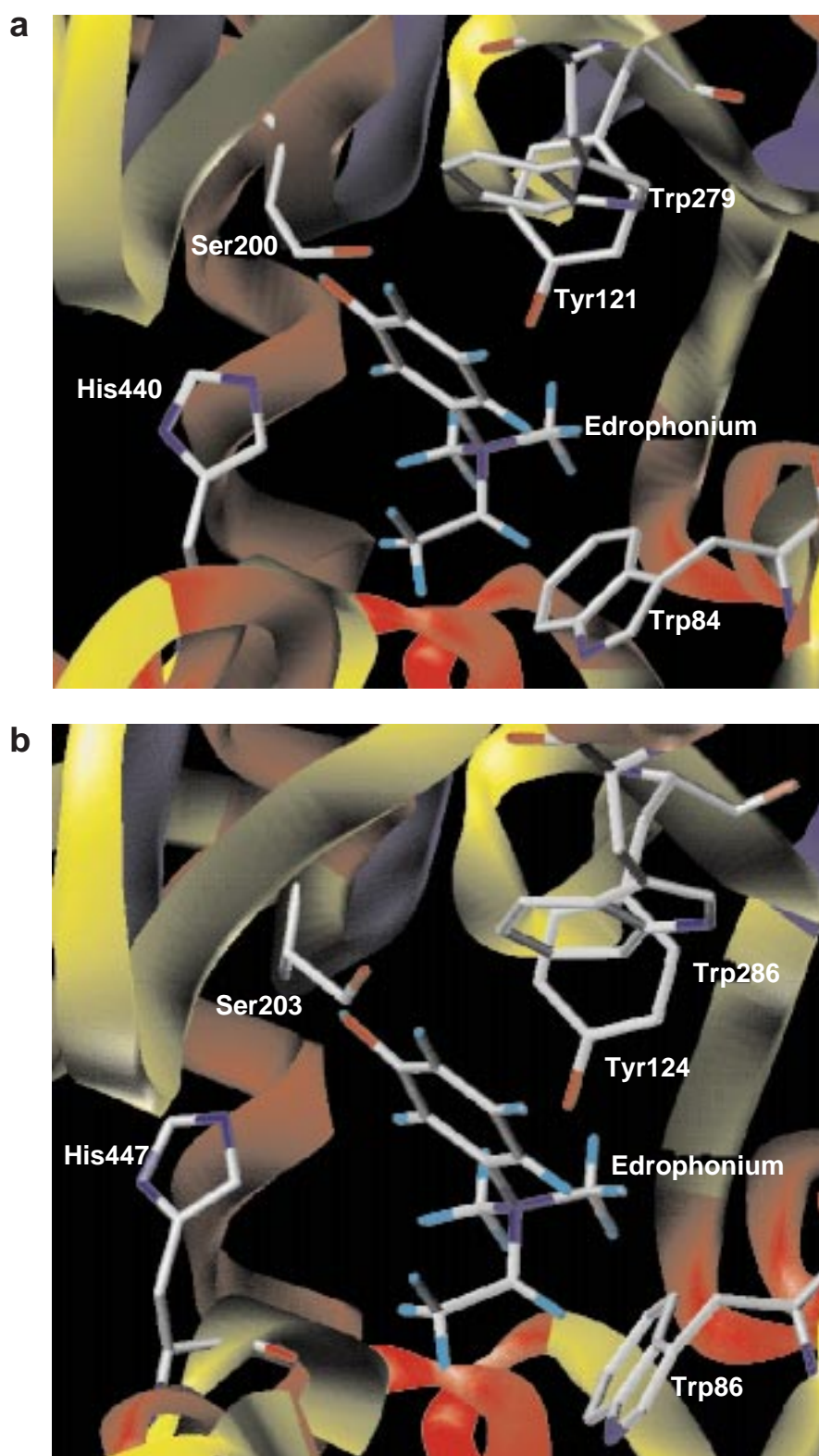


*Figure 1.* Complex of TAcHe with edrophonium: (a) the observed one, and (b) the virtual complex of the mouse acetylcholinesterase with a projected edrophonium molecule.

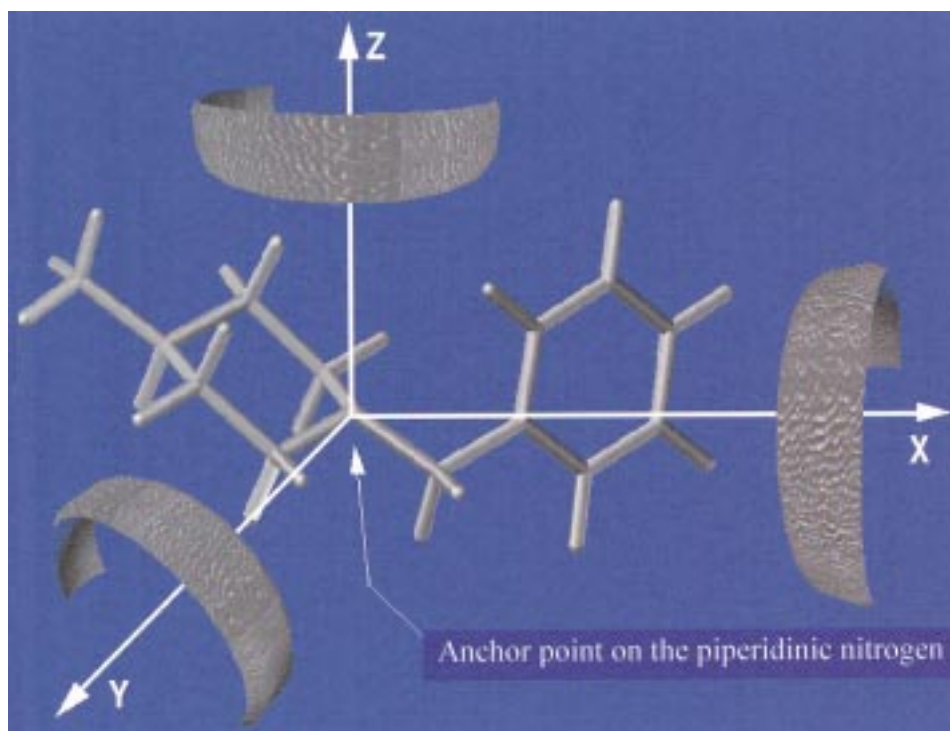


*Figure 2.* The automated docking procedure. The piperidinic nitrogen was projected in place of the edrophonium's quaternary nitrogen. This position was used as an anchor point for rotations of the molecules studied around the X, Y and Z axes. A conformational search was performed at each orientation of the molecule.

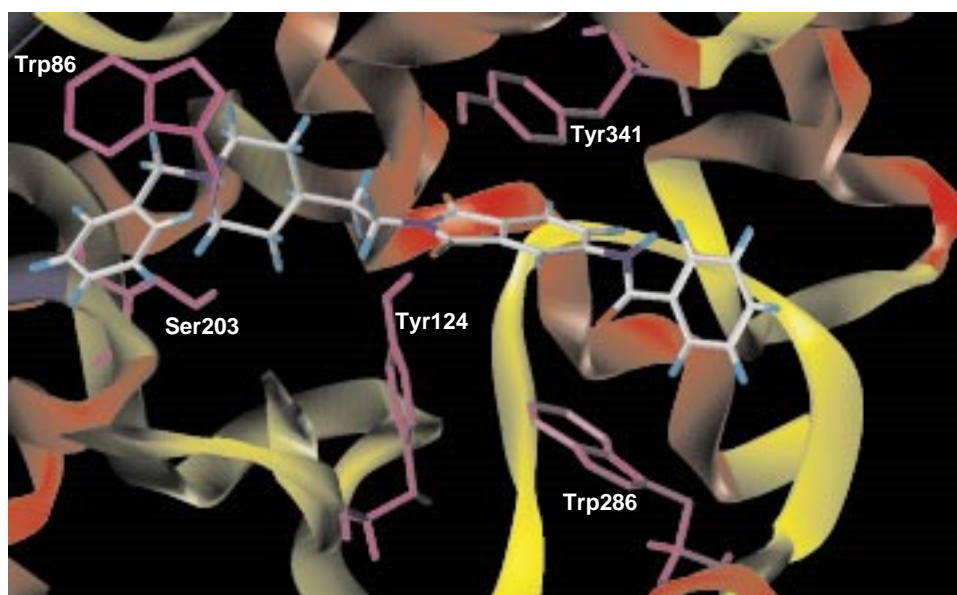


*Figure 3.* Compound **48** docked to MACH.

[25]. The lowest energy conformations were found by means of the SYBYL/SEARCH option and then used as initial conformations for docking. As the enzymatic measurements for these *N*-benzylpiperidine derivatives were taken at pH = 8, the compounds were considered in their protonated forms.

*Ligand-enzyme docking.* Each ligand was placed into the enzyme with the piperidinic nitrogen fixed as described above. The ligand was then rotated around the three coordinate axis as shown in Figure 2 with a step of 30°. These reorientations were performed by means of the SYBYL/SYSTEMATIC SEARCH option. To this end, a chain of four atoms of type 'any' was attached to the anchor nitrogen. The parameters of the 'any' atom were modified in order to make it completely transparent for the energy calculation algorithm. The valence angles of type 'any-any-any' and the torsion angles of type 'any-any-any-P' and 'any-any-any-any' were set to 90°. The systematic search procedure was applied to all rotatable bonds of the ligand including the bonds of the attached chain (the procedure was not however applied to the rotatable bonds of the protein). The rotation steps for the rotatable bonds of the ligand were also fixed at 30°. The number of rotated bonds for some ligands was up to 12. The conformations of the ligand having bad steric interactions with the protein were eliminated at the first fast step of search procedure prior to energy calculations. This fast procedure is a part of Sybyl's search algorithm which is based on estimating the overlap between the atomic van der Waals spheres. The adjustable threshold of this overlap can be used to eliminate greater or smaller number of 'bad' complexes. At the second step of the search procedure, the energy of the enzyme-ligand complex was calculated for each ligand's conformation and orientation within the protein. Usually we allowed a 30% overlap between the van der Waals radii that resulted in up to several hundreds of complexes with calculated energies. The computational times for complexes with 10–12 rotatable bonds were 30–50 min on an SGI Indy 5000, 150 MHz. The ligand conformers extracted from their complexes were then clustered by means of the Sybyl clustering algorithm, which resulted in up to 10 clusters (conformational families). The lowest energy conformers from each family were selected to refine the enzyme-ligand complexes by the systematic search with a step of 5° in the interval of  $\pm 30^\circ$  around the torsion values of this conformer. These refined enzyme-ligand complexes were optimised using

the Tripos force field. Both ligand and enzyme were fully relaxed during this optimisation. However, neither the ligand geometry nor the enzyme one were significantly changed in the course of optimisation because of the fore-mentioned refinement procedure. The lowest energy inhibitor geometries were then used in the CoMFA analysis.

### CoMFA

*Data set.* The training set and corresponding biological data used in this study were selected from literature [9, 10]. The molecular structures and AChE inhibitory activity data of 82 benzylpiperidine derivatives are summarized in Tables 1, 2 and 3. All collected biological data were measured under the same experimental conditions on MACHÉ.

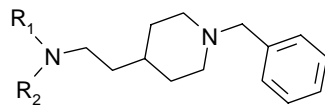
A new series of 29 *N*-benzylpiperidine benzisoxazole derivatives [26], whose structure and activity data are presented in Table 4, was involved in the validation of the CoMFA model. The QSAR/ANALYSIS/PREDICT option of SYBYL was used to calculate the AChE inhibitory activity for these compounds.

*CoMFA method.* A CoMFA study normally begins with searching for a suitable alignment of the molecules under investigation by using a constrained reference compound. In the present study this problem was a priori resolved by docking the compounds to the crystal AChE structure.

Both steric and electrostatic CoMFA fields were calculated using an  $sp^3$  carbon atom as a probe, with a charge of +1 in the grid points around the molecules. The grid points were spaced by 1.0 Å in all three dimensions. Partial atomic charges for the electrostatic field calculation were obtained by the MOPAC AM1 method [27]. The CoMFA region was chosen to include all the molecules with margins of at least 4.0 Å. A default value of 30 kcal/mol was chosen as a cutoff for the electrostatic CoMFA field.

The partial least squares method (PLS) [28] was used to linearly relate the CoMFA fields to the inhibitory activity values. The optimal number of PLS components was determined using the 'leave-one-out' cross-validation procedure [28]. The model quality is expressed in terms of  $Q^2$  (cross-validated correlation coefficient),  $R^2$  (conventional correlation coefficient),  $s$  (standard error) and  $F$  (Fisher test).

Table 1. In vitro inhibition of AChE by *N*-benzylpiperidine derivatives

				
Compd no.	R <sub>1</sub>	R <sub>2</sub>	IC <sub>50</sub> (nM)	log (1/IC <sub>50</sub> ) (μM)
1	PhCO	H	560.0	0.25
2	<i>o</i> -CH <sub>3</sub> PhCO	H	1000.0	0.00
3	<i>m</i> -CH <sub>3</sub> PhCO	H	470.0	0.33
4	<i>p</i> -CH <sub>3</sub> PhCO	H	180.0	0.74
5	<i>o</i> -NO <sub>2</sub> PhCO	H	880.0	0.06
6	<i>m</i> -NO <sub>2</sub> PhCO	H	230.0	0.64
7	<i>p</i> -NO <sub>2</sub> PhCO	H	55.0	1.26
8	<i>p</i> -OCH <sub>3</sub> PhCO	H	88.0	1.06
9	<i>p</i> -CHOPhCO	H	120.0	0.92
10	<i>p</i> -ClPhCO	H	180.0	0.74
11	<i>p</i> -FPhCO	H	85.0	1.07
12	<i>p</i> -CH <sub>3</sub> COPhCO	H	51.0	1.29
13	<i>p</i> -(PhCH <sub>2</sub> SO <sub>2</sub> ) PhCO	H	29.0	1.54
14	<i>o</i> -pyridineCO	H	800.0	0.10
15	<i>m</i> -pyridineCO	H	69.0	1.16
16	<i>p</i> -pyridineCO	H	39.0	1.41
17	C <sub>6</sub> H <sub>11</sub> CO	H	1600.0	−0.20
18	PhCH <sub>2</sub>	H	46000.0	−1.66
19	PhCO	CH <sub>3</sub>	170.0	0.77
20	PhCO	C <sub>2</sub> H <sub>5</sub>	130.0	0.89
21	PhCO	PhCH <sub>2</sub>	940.0	0.03
22	PhCO	Ph	35.0	1.46
23	<i>p</i> -(PhCH <sub>2</sub> SO <sub>2</sub> ) PhCO	CH <sub>3</sub>	0.6	3.22
24	<i>p</i> -(PhCH <sub>2</sub> SO <sub>2</sub> ) PhCO	C <sub>2</sub> H <sub>5</sub>	0.3	3.52
25	<i>p</i> -(PhCH <sub>2</sub> SO <sub>2</sub> ) PhCO	Ph	0.6	3.22
26	<i>p</i> -OCH <sub>3</sub> PhCO	Ph	590.0	0.23
27	<i>p</i> -FPhCO	Ph	18.0	1.74
28	<i>p</i> -NO <sub>2</sub> PhCO	Ph	5.4	2.27
29	<i>p</i> -pyridineCO	Ph	64.0	1.19
30	C <sub>6</sub> H <sub>11</sub> CO	Ph	9400.0	−0.97
31	CH <sub>3</sub> CO	Ph	52.0	1.28
32	CH <sub>3</sub> CH <sub>2</sub> CO	Ph	830.0	0.08
33	CH <sub>3</sub> CO	<i>m</i> -OCH <sub>3</sub> Ph	46.0	1.34
34	CH <sub>3</sub> CO	<i>p</i> -OCH <sub>3</sub> Ph	700.0	0.15
35	CH <sub>3</sub> CO	<i>m</i> -FPh	65.0	1.19
36	CH <sub>3</sub> CO	<i>p</i> -FPh	205.0	0.69
37	CH <sub>3</sub> CH <sub>2</sub>	Ph	12000.0	−1.08
38	CH <sub>3</sub> CO	<i>p</i> -pyridine	108.0	0.97
39	CH <sub>3</sub> CO	CH <sub>3</sub>	660.0	0.18



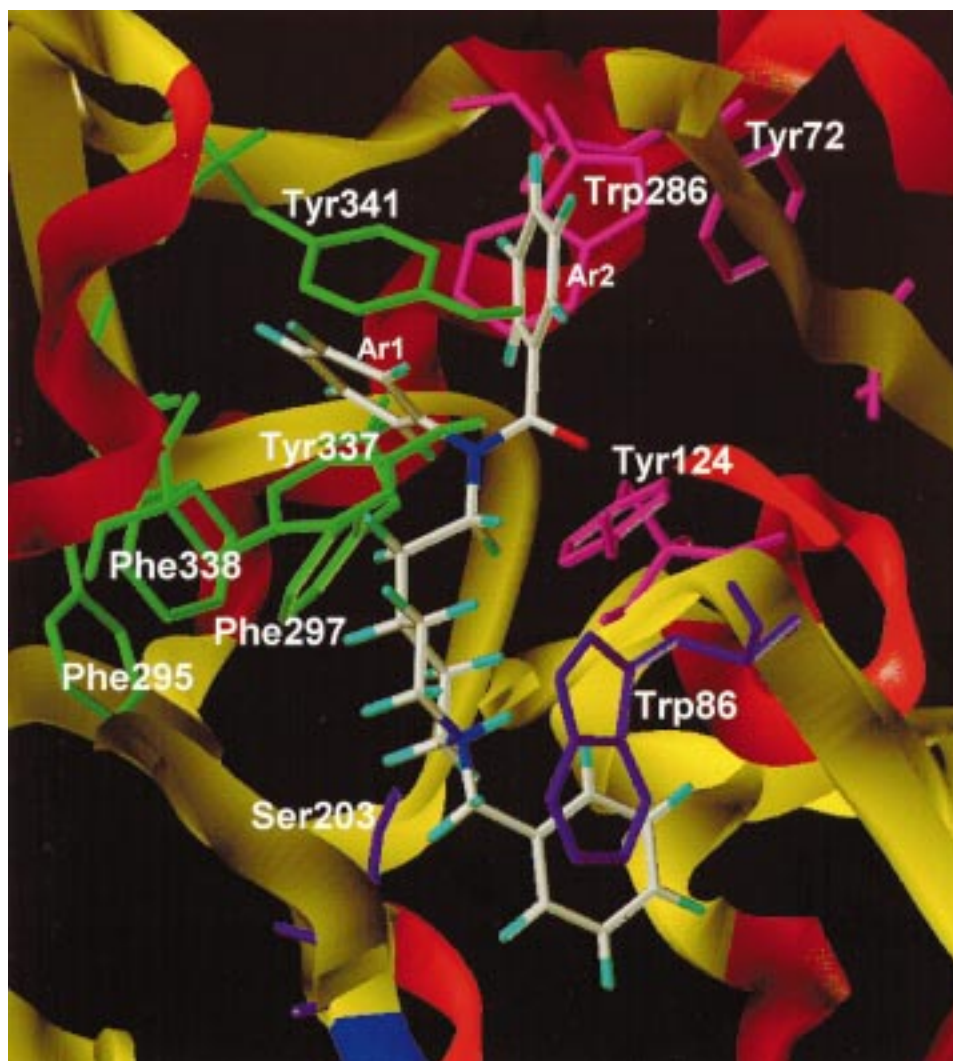


Figure 4. Compound **22** docked to the MACH residues susceptible to have hydrophobic interactions, with the Ar1 and Ar2 fragments of the inhibitor. These residues are shown in green and in magenta, respectively.

## Results and discussion

### Docking

In the present section, a few key inhibitor structures that demonstrate the most characteristic ligand-protein interactions will be discussed. In general, it may be evidenced that the inhibitors take an unfolded shape and form a bridge between the ‘anionic’ (Trp86) and ‘peripheral’ (Trp286) sites of AChE (see Figure 3). While the *N*-benzylpiperidine moiety neighbors the ‘anionic site’, the phthalimido group and its derivatives are localized close to the ‘peripheral site’. A thorough probing inside the protein by means of our automated docking routine shows that these inhibitors

would in no way be able to adopt a different orientation. These results are in agreement with the concept of a ‘deep and narrow gorge’, issued from the crystallographic study [29]. The most potent inhibitors, e.g. compounds **24**, **48**, are the longest ones. This suggests that these inhibitors have favorable electrostatic and hydrophobic interactions throughout the gorge. Compound **24** is, for example, 23.5 Å long, and its terminal phenyl group is located close to the protein surface.

This study also suggests attractive interactions between the carboxyl oxygens of the phthalimido group featuring many compounds of the series and the residues of the ‘peripheral site’. For example, compounds **42**, **45–55** form a hydrogen bond with Tyr124.



Table 2. In vitro inhibition of AChE by *N*-benzylpiperidine derivatives

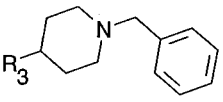
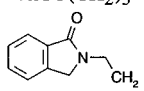
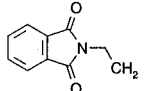
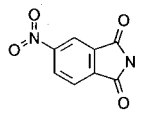
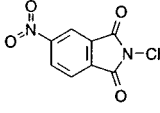
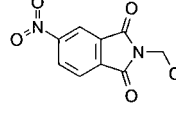
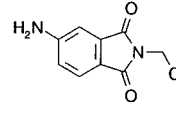
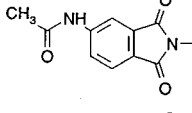
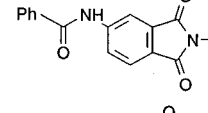
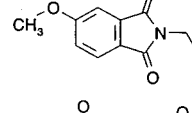
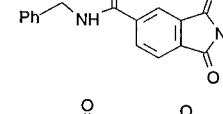
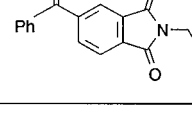
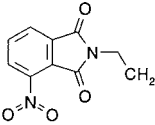
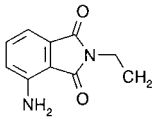
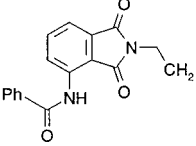
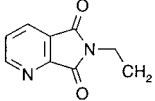
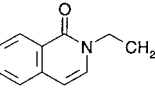
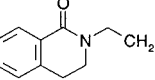
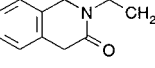
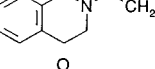
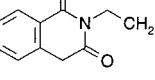
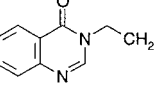
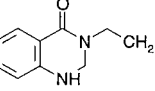
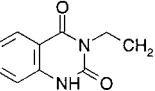
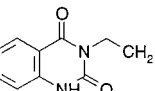
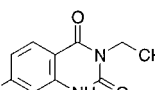
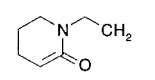
			
Compd no.	R <sub>3</sub>	IC <sub>50</sub> (nM)	log (1/IC <sub>50</sub> ) (μM)
40	PhCO(CH <sub>2</sub> ) <sub>3</sub>	530.0	0.28
41		98.0	1.01
42		30.0	1.52
43		27000.0	-1.43
44		3000.0	-0.48
45		12.5	1.90
46		8.8	2.06
47		2.8	2.55
48		1.2	2.92
49		8.0	2.10
50		2.2	2.66
51		2.4	2.62

Table 2. (continued)

Compd no.	R <sub>3</sub>	IC <sub>50</sub> (nM)	log (1/IC <sub>50</sub> ) (μM)
52		9.0	2.05
53		11.0	1.96
54		340.0	0.47
55		13.0	1.89
56		1100.0	-0.04
57		1000.0	0.00
58		17.0	1.77
59		1600.0	-0.20
60		23.0	1.64
61		1200.0	-0.08
62		800.0	0.10
63		4.2	2.38
64		13.0	1.89
65		4.5	2.35
66		270.0	0.57

The binding of the phthalimido group to residues of the enzyme may also explain why the absence of such a group decreases the activity. The congeneric compounds **56**, **57**, **59**, **61**, **62**, which are not able to create a H-bonds, are not active. Moreover, the substituents attached to the phthalimido moiety in compounds **47–51** seem to form one more hydrogen bond with Tyr72 owing to their H-bond acceptor groups, while the phthalimido nucleus has a  $\pi$ - $\pi$  interaction with Tyr341 at about 3.5 Å from it. The ‘peripheral’ and ‘catalytic’ sites of MACHC complexed with compound **48** are presented in Figure 3.

The hypothesis on the hydrogen bond with Tyr124 is also supported by another subset of compounds which possess a tertiary amino instead of the phthalimido group. Compound **22**, a potent inhibitor, has at least three attractive sites which interact with the residues of the ‘peripheral’ site. The strongest of these sites, i.e. the carbonyl oxygen, forms a hydrogen bond with Tyr124, as shown in Figure 4. This hydrogen bond is indispensable for the inhibitory activity. Indeed, compounds **18** and **37**, which do not possess an acceptor group interacting with Tyr124, are inactive. Two other sites, i.e. two phenyl groups, one attached to the carbonyl group and another to the amino nitrogen, do not seem to be not so crucial. The absence of one of these groups in congeneric compounds **19** and **31** provokes only a slight decrease in activity. However, the absence of both phenyl groups in compound **39** results in a significant 10-fold decrease in activity. Both phenyl moieties are located in a lipophilic environment and are exposed to attractive lipophilic interactions with the neighbouring protein residues. The phenyl fragment attached to the carbonyl group probably interacts with Tyr72, Tyr124 and Trp286. Another phenyl fragment is stabilized by the presence of lipophilic Phe295, Phe297, Tyr337, Phe338, Tyr341. The correlation between the ligand-enzyme interaction model suggested and the activity variation for compounds **18**, **19**, **22**, **31**, **37** and **39** strongly supports the validity of the automated docking procedure presented.

Unlike the compounds reported by the previous docking papers [11–14], many inhibitors studied here (compounds **21**, **22**, **25–37**) possess aromatic fragments intervening into the aforementioned domain {Phe295, Phe297, Tyr337, Phe338, Tyr341} which was not touched by the compounds studied earlier. This domain is crucial for the enzymatic activity, because it makes a difference between AChE and butyrylcholinesterase [30, 31].

An analogy between compounds **41–55** that possess phthalimido groups and compounds **1–39** having amido groups is not limited to the aforementioned hydrogen bond with Tyr124. Indeed, compounds **12–13**, **23–25** are also bound to Tyr72, in the same way as phthalimidic compounds **47–51**. This hydrogen bond leads to a remarkable growth of their inhibitory activity, especially for compounds **23–25** which are the most potent AChE inhibitors among the 82 benzylpiperidines studied.

Concerning the benzylpiperidine moiety, no substituents are really able to increase inhibitory activity. For example, in the *para* position all substituents lead to a decrease in activity (see compounds **69**, **72**, **80** and **81**). This could be explained by the presence of residues Tyr119, Gly120 and Leu130 close to the *para* hydrogen of the benzyl group.

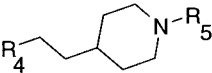
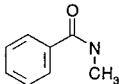
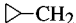
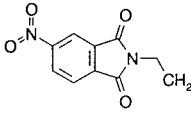
### CoMFA

The present CoMFA study is particular in that each of the 82 benzylpiperidines studied was aligned in an independent way. No reference compound was used and the geometries of the inhibitors were only determined by interactions with the biological receptor. The automated docking study showed that, despite a great flexibility of the molecules studied, the choice of the suitable conformations was not ambiguous. Indeed, in most cases the conformational search yielded only a single conformation (or a single conformational family) for the ligand-protein complex whose energy was much lower than that of the other candidate complexes. Hence, it may be suggested that the gorge of the protein is quite narrow and does not permit the conformational mobility of the bound inhibitor.

The natural alignment without a reference compound may have an impact on the nature of the structural information which we expect to obtain from the CoMFA analysis. In the present case, the good quality of the CoMFA model would suggest the validity of the proposed model of inhibitor-enzyme interactions obtained by the automated docking procedure.

During this CoMFA study, we obtained some unexpected evidence that supported the necessity of docking all the compounds of the training set to the receptor structure. In fact, the initial plan was to dock only representative active compounds, and then to use the representatives as reference compounds, and fit all the others to the references. Following that, we obtained a CoMFA model of satisfactory quality ( $Q^2 = 0.48$ ) with a number of outliers. All these outliers

Table 3. In vitro inhibition of AChE by *N*-piperidine derivatives

				
Compd no.	R <sub>4</sub>	R <sub>5</sub>	IC <sub>50</sub> (nM)	log (1/IC <sub>50</sub> ) (μM)
67		<i>o</i> -CH <sub>3</sub> Bzl	770.0	0.11
68	id	<i>m</i> -CH <sub>3</sub> Bzl	145.0	0.84
69	id	<i>p</i> -CH <sub>3</sub> Bzl	41000.0	-1.61
70	id	<i>o</i> -NO <sub>2</sub> Bzl	14000.0	-1.15
71	id	<i>m</i> -NO <sub>2</sub> Bzl	370.0	0.43
72	id	<i>p</i> -NO <sub>2</sub> Bzl	3300.0	-0.52
73	id	PhCH <sub>2</sub> CH <sub>2</sub>	13000.0	-1.11
74	id	PhCH=CHCH <sub>2</sub>	54000.0	-1.73
75	id	PhCO	52000.0	-1.72
76	id	H	26000.0	-1.41
77	id	 -CH <sub>2</sub>	38000.0	-1.58
78	id	C <sub>6</sub> H <sub>11</sub> CH <sub>2</sub>	410.0	0.39
79	id	adamantylCH <sub>2</sub>	24000.0	-1.38
80		<i>p</i> -CH <sub>3</sub> O Bzl	440.0	0.36
81	id	<i>p</i> -Cl Bzl	240.0	0.62
82	id	CH <sub>3</sub>	6800.0	-0.83

(compounds **1**, **7**, **16**, **26**, **30**, **31**, **60**, **69**, **70**, **79**) were not directly docked to the protein but fitted to the reference compounds. After docking all the compounds to the protein, a model with no outliers was obtained. The discussion on a CoMFA model thus improved is given in the following sections.

For a better understanding of the factors which underlie the activity, three different CoMFA models were built: (i) a model with steric field only; (ii) a model with electrostatic field; and (iii) a model taking both fields into account. The results of these analyses are presented in Table 5. Because of the large number of compounds, the number of principal components (PC) selected by the cross-validation routine was also high. The diagram in Figure 5 shows the evolution of the squared cross-validated correlation coefficient ( $Q^2$ ) with the growth of the number of PC. On the diagram,  $Q^2$  increases up to 10 PC. However, at 7 PC the curve is bending. Starting from this point, the growth of  $Q^2$  is very weak. Hence, for all the three CoMFA

analyses the models based on 7 principal components were taken for further discussion.

Table 5 underlines the important role of the CoMFA electrostatic field compared to that of the steric field. Indeed, the analysis including both fields shows that the relative contributions to the model are 33.2% for the steric field and 66.8% for the electrostatic one. Moreover, the statistic and predictive criteria for the analysis including steric field are significantly lower than the corresponding criteria for the other two analyses. Such a superiority of the electrostatic contribution means, however, that the process of the AChE inhibition is mainly guided by electrostatic forces. It only expresses the structural variation in the training set. In the present study, the model comprising both steric and electrostatic fields ( $Q^2 = 0.75$ ) was finally taken to plot the CoMFA statistic fields and to predict the AChE inhibitory activity for new compounds.

Finally, a non cross-validated PLS run was performed in order to generate the final CoMFA plots.

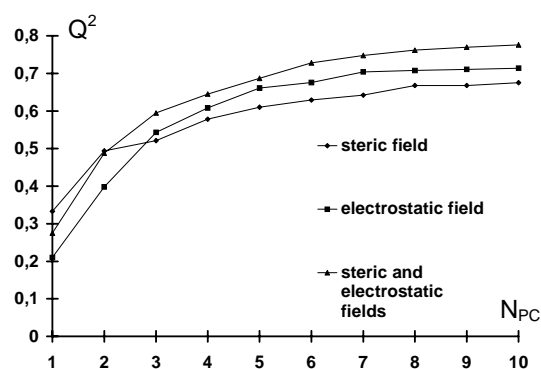


Figure 5.  $Q^2$  values for three CoMFA models plotted versus number of PLS components.

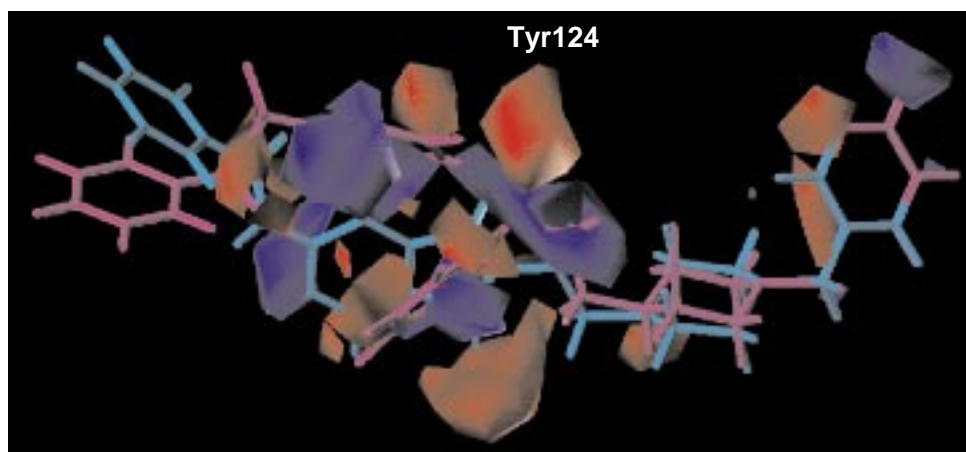


Figure 6. CoMFA electrostatic STDEV\*COEFF field plot. Increasing negative charge inside red regions and increasing positive charge in blue regions favors the inhibitory activity. Compounds **22** and **48** are shown in magenta and cyan, respectively.

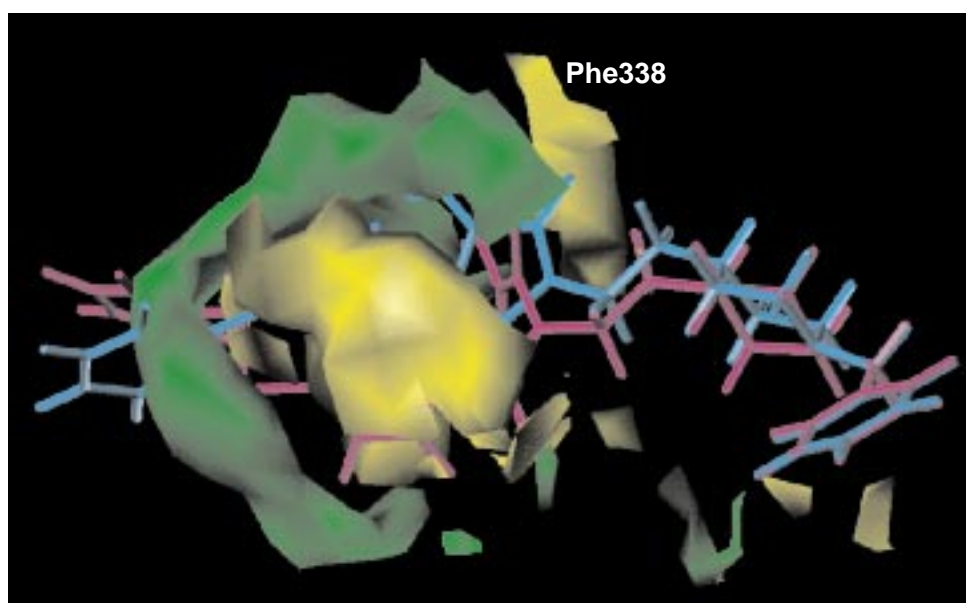


Figure 7. CoMFA steric STDEV\*COEFF field plot. Increasing bulk inside green regions and removing bulk from yellow regions favours the inhibitory activity. Compounds **22** and **48** are shown in magenta and cyan, respectively.

Table 4. Human in vitro inhibition of AChE by *N*-benzylpiperidine-benzisoxazoles and their log (1/IC<sub>50</sub>) calculated with the CoMFA model based on both steric and electrostatic contributions

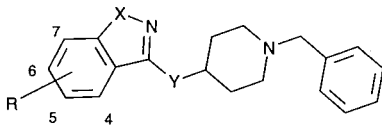
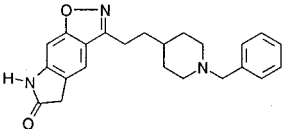
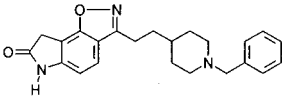
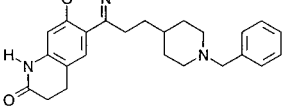
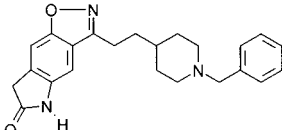
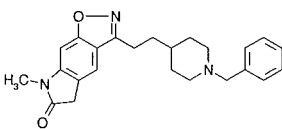
						
Compd no.	R	X	Y	IC <sub>50</sub> (nM)	log (1/IC <sub>50</sub> ) <sub>obs</sub>	log (1/IC <sub>50</sub> ) <sub>pred</sub>
83	H	O	(CH <sub>2</sub> ) <sub>2</sub>	55.00	1.26	0.30
84	5-Me	O	(CH <sub>2</sub> ) <sub>2</sub>	7.80	2.11	0.62
85	5, 6-diMe	O	(CH <sub>2</sub> ) <sub>2</sub>	5.80	2.24	0.19
86	5-OMe	O	(CH <sub>2</sub> ) <sub>2</sub>	7.20	2.14	0.50
87	6-OMe	O	(CH <sub>2</sub> ) <sub>2</sub>	8.30	2.08	0.23
88	7-OMe	O	(CH <sub>2</sub> ) <sub>2</sub>	7.10	2.15	0.17
89	6-NHCOMe	O	(CH <sub>2</sub> ) <sub>2</sub>	2.80	2.55	0.86
90	6-NHCOPh	O	(CH <sub>2</sub> ) <sub>2</sub>	9.40	2.03	0.81
91	6-NHSO <sub>2</sub> Ph	O	(CH <sub>2</sub> ) <sub>2</sub>	14.00	1.85	0.30
92	6-N $\begin{smallmatrix} \text{---} \text{N} \text{---} \text{O} \end{smallmatrix}$	O	(CH <sub>2</sub> ) <sub>2</sub>	0.80	3.10	0.93
93	6-NH <sub>2</sub>	O	(CH <sub>2</sub> ) <sub>2</sub>	20.00	1.70	0.07
94	6-OH	O	(CH <sub>2</sub> ) <sub>2</sub>	26.00	1.59	0.14
95	6-Br	O	(CH <sub>2</sub> ) <sub>2</sub>	50.00	1.30	0.20
96	6-CN	O	(CH <sub>2</sub> ) <sub>2</sub>	101.00	1.00	-0.01
97	6-CONH <sub>2</sub>	O	(CH <sub>2</sub> ) <sub>2</sub>	8.80	2.06	0.70
98	H	O	(CH <sub>2</sub> ) <sub>3</sub>	900.00	0.05	-0.94
99	H	O	E-CH=CH	210.00	0.68	-0.01
100	H	O	O-CH <sub>2</sub>	2600.00	-0.41	-0.58
101	H	O	NH-CH <sub>2</sub>	320.00	0.49	-0.07
102	H	O	NH-(CH <sub>2</sub> ) <sub>2</sub>	810.00	0.09	-0.32
103	H	S	(CH <sub>2</sub> ) <sub>2</sub>	99.00	1.05	0.22
104	H	CH=CH	(CH <sub>2</sub> ) <sub>2</sub>	220.00	0.66	-0.24
105	H	N=CH	(CH <sub>2</sub> ) <sub>2</sub>	340.00	0.47	-0.28
106	H	NH	(CH <sub>2</sub> ) <sub>2</sub>	120.00	0.92	0.28
107		—	—	0.33	3.48	1.08
108		—	—	3.60	2.44	0.48
109		—	—	0.57	3.24	0.75
110		—	—	0.95	3.02	0.59
111		—	—	0.48	3.32	1.24



Table 5. Statistics and cross-validation results of the three CoMFA models

	Steric	Electrostatic	Steric and electrostatic
N		82	
npC		7	
Q <sup>2</sup>	0.64	0.70	0.75
R <sup>2</sup>	0.93	0.98	0.98
F	138	434	508
sd	0.36	0.21	0.19

These plots outline a CoMFA statistic field which expresses the relationship between the variation of the steric and electrostatic fields and the variation of the biological activity. The values of the field are calculated at each lattice intersection and are equal to the product of the descriptor coefficient by the corresponding standard deviation (STDEV\*COEFF). Hence, an extremely low value of STDEV\*COEFF indicates that the presence of the corresponding steric or electrostatic field is not desirable in this point because this provokes a decrease in activity. New molecules should not contain fragments that generate such a field in the lattice intersections with low STDEV\*COEFF. A high value of STDEV\*COEFF means that the corresponding field is desirable in this point and the presence of fragments that produce such a field favors the activity. A STDEV\*COEFF plot for the electrostatic field is shown in Figure 6 and a plot for the steric field is presented in Figure 7.

Two active compounds, **25** and **48**, of the training set illustrate the main features of the CoMFA plots. Some of the colored regions on the plots mark essential ligand-protein interactions. For instance, a red sphere that envelopes the carbonyl oxygen of the phthalimido moiety of the inhibitor suggests there is always a negatively charged inhibitor group in the region. This negatively charged group is able to form a hydrogen bond with Tyr124. The green surface in Figure 7 surrounding the phthalimido moiety of compound **48** and the phenyl ring of compound **25** is in favor of attachment of bulky substituents to these moieties. A bulky substitution is also possible at the *meta* position of the benzyl group of the benzylpiperidine moiety. The region around this *meta* position is also favorable to the negatively charged substituents. On the other hand, a *para* substitution is fatal to the activity that is supported by the corresponding yellow zone. Substitutions are also sterically unfavorable near

the carbonyl group interacting with Tyr124 and near Trp286. Another yellow zone corresponds to the presence of Phe338. This explains why some molecules having substituents in this zone are not active.

#### Predictive aspect of the CoMFA model

After validating our model by means of cross-validation, the next step of the investigation consisted in applying the model to inhibitors whose activity values were measured under experimental conditions which differed from the conditions in which the compounds of the training set were tested. The compounds of the training set were tested on mouse AChE with a preincubation time of 60 min [9, 10] and the 29 compounds of the novel series were tested on human AChE with a preincubation time of 20 min [14, 26]. Because of this difference in testing conditions, the series of 29 compounds could have been considered as ineligible for the training set.

The purpose of this step was to validate the model and simultaneously to explore the area of its applicability. Another important issue addressed was the compatibility between the data measured under different experimental conditions. A variety of approaches to this problem may be found in the literature. In a recent CoMFA study [15], the data measured on two different proteins (mouse and human AChE) were dried both in the same training set and in separate sets. CoMFA models of comparable quality were obtained in both cases. In the latest source [16], special care was taken to provide compatibility. All the data were measured on the same enzyme, from *Torpedo californica*, and two reference compounds were used to prove compatibility of the data.

However, using one or two reference compounds cannot completely justify merging different series. For example, in the experimental study [9], the AChE inhibitory activity (IC<sub>50</sub>) of tacrine is 81 nM. In another study [26] the activity of tacrine is 170 nM, i.e., relatively close to 81 nM. It may be concluded that the data from these two sources are compatible. Nevertheless, using physostigmine as a reference compound leads to a much less optimistic conclusion. Physostigmine has an AChE activity of 0.69 nM in one of the studies [9] and 19 nM in another study [13], which makes a 28-fold difference between the values. One may argue that some experimental parameters in the two aforementioned studies were different and that taking data measured under the same conditions would ensure compatibility, whatever the laboratory issuing

the data may be. Experience shows, however, that the experimental conditions in different laboratories are rarely the same [9, 14, 32, 33]. More specifically, the combination of four, most important, experimental parameters such as enzymatic assay methodology, source of enzyme, pH level and preincubation time differs from one laboratory to another.

Structural formulas, predicted and real activity values with corresponding deviations for the above 29 benzylpiperidines are shown in Table 4. The plot in Figure 8 illustrates how tightly the predicted values are correlated with the actual activity values ( $r = 0.90$ ). It means that the relative inhibitory capacities are correctly predicted for the whole series of 29 molecules. However, a parameter which is widely used to estimate the quality of test set predictions, i.e. PRESS/SSY [34], has a high value of 0.6, which can be related to systematic deviations of the predicted values from the actual ones. A good correlation with simultaneous large deviations indicates a significant linear shift of the predicted data. The following equation relates both observed and predicted activity values:

$$\log(1/IC_{50})_{\text{pred}} = 0.52 \log(1/IC_{50})_{\text{obsd}} - 0.59, \quad (1)$$

$n = 29, r = 0.90, s = 0.47, F = 113$

Two conclusions may be derived from this part of the study. First, the tight correlation between the predicted and experimentally observed values in this study suggests that the present model is able to provide reliable predictions of the *relative* AChE inhibitory capacities in a set of new inhibitors. The good correlation between predicted and observed values also indicates a good predictive capacity of the present CoMFA model. The second conclusion is that the shift of the predictions for these 29 compounds provides a supplementary argument for taking more care when selecting a training set. More specifically, data should be collected from the same laboratory source.

## Conclusions

An automated docking study was performed on a series of potent, reversible AChE inhibitors susceptible to be potential drugs against Alzheimer's disease. Spatial constraints issued from the crystallographic data were initially imposed in order to reduce the searchable space. Due to the constraints, reliable docking was performed for all the 82 molecules studied with reasonable computational expenses.

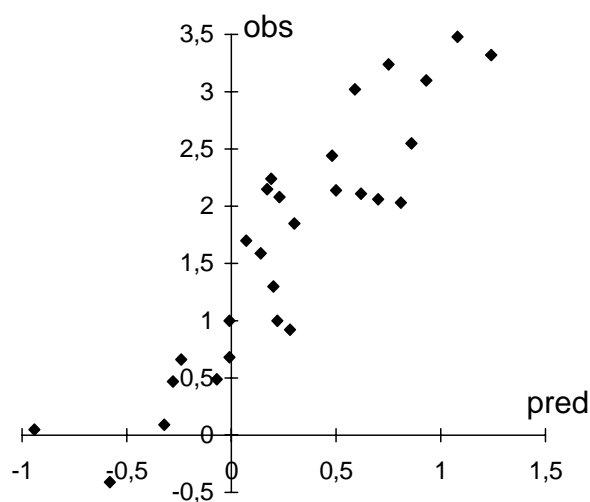


Figure 8. Experimental versus predicted inhibitory activity values on human AChE for 29 *N*-benzylpiperidines.

The present work is in agreement with some earlier studies on the existence of an 18–20 Å long pocket receiving the inhibitors. It was shown that the pocket is quite narrow and does not allow these inhibitors conformational flexibility. The most potent inhibitors tend to form hydrogen bonds with Tyr124 and Tyr72. Stabilizing hydrophobic interactions were observed with Phe295, Phe297, Tyr337, Phe338 and Tyr341.

The docking data were then used to proceed with the Comparative Molecular Field Analysis. The CoMFA model with the 'natural' alignment has a high predictive capacity according to the cross-validation test. The CoMFA plots are in agreement with the docking results and should be of use for the design of new effective inhibitors.

An independent series of 29 *N*-benzylpiperidines, whose AChE activities were measured under different experimental conditions, was used to study the area of the model applicability. The relative inhibitory capacities were correctly predicted for all 29 molecules.

This robust and predictive model of the AChE inhibitory activity might further be used for the selection of new active molecules and would also witness the validity of the conformations obtained by the docking study. Such a feedback creates a synergy between the receptor-based and QSAR approaches.

## Acknowledgements

The 'Fondation pour la Recherche Médicale' is acknowledged for a grant to one of us (P.B.).

## References

- Rosser, M.N., Iversen, L.L., Reynolds, G.P., Mountjoy, C.A. and Roth, M., *Br. Med. J.*, 288 (1984) 961.
- Barnard, E.A., In Hubbard, J.I. (Ed.) *The Peripheral Nervous System*, Plenum, New York, NY, 1974, pp. 201–224.
- Sims, N.R., Bowen, D.M., Allen, S.J., Smith, C.C.T., Neary, D., Thomas, D.J. and Davison, A.N., *J. Neurochem.*, 40 (1983) 503.
- Perry, E.K., *Br. Med. Bull.*, 42 (1986) 408.
- Becker, R.E. and Giacobini, E., *Drug Dev. Res.*, 12 (1988) 163.
- Johns, C.A., Haroutunian, V., Greenwald, B.S., Mohs, R.C., Davis, B.M., Kanof, P., Horvath, T.B. and Davis, K.L., *Drug Dev. Res.*, 5 (1985) 77.
- Brennan, M.B., *Chem. Eng. News*, 20 (1997) 29.
- John, V., Lieberburg, I. and Thorsett, E.D., *Annu. Rep. Med. Chem.*, 28 (1993) 197.
- Sugimoto, H., Tsuchiya, T., Sugumi, H., Higurashi, K., Karibe, N., Iimura, Y., Sasaki, A., Kawakami, Y., Nakamura, T., Araki, S., Yamanishi, Y. and Yamatsu, K., *J. Med. Chem.*, 33 (1990) 1880.
- Sugimoto, H., Tsuchiya, T., Sugumi, H., Higurashi, K., Karibe, N., Iimura, Y., Sasaki, A., Kawakami, Y., Araki, S., Yamanishi, Y. and Yamatsu, K., *J. Med. Chem.*, 35 (1992) 4542.
- Pang, Y.-P. and Kozikowski, A.P., *J. Comput.-Aided Mol. Design*, 8 (1994) 683.
- Yamamoto, Y., Ishihara, Y. and Kuntz, I.D., *J. Med. Chem.*, 37 (1994) 3141.
- Inoue, A., Kawai, T., Wakita, M., Iimura, Y., Sugimoto, H. and Kawakan, Y., *J. Med. Chem.*, 39 (1996) 4460.
- Villalobos, A., Blake, J.F., Biggers, C.K., Butler, T.W., Chapin, D.S., Chen, Y.L., Ives, J.L., Jones, S.B., Liston, D.R., Nagel, A.A., Nason, D.M., Nielsen, J.A., Shalaby, I.A. and Frost White, W., *J. Med. Chem.*, 37 (1994) 2721.
- Tong, W., Collantes, E.R., Chen, Y. and Welsh, W.J., *J. Med. Chem.*, 39 (1996) 380.
- Cho, S.J., Serrano Garsia, M.L., Bier, J. and Tropsha, A., *J. Med. Chem.*, 39 (1996) 5064.
- Cardozo, M.G., Imura, Y., Sugimoto, H., Yamanishi, Y. and Hopfinger, A.J., *J. Med. Chem.*, 35 (1992) 584.
- Kuntz, I.D., Meng, E.C. and Shoichet, B.K., *Acc. Chem. Res.*, 27 (1994) 117.
- Cramer III, R.D., Patterson, D.E. and Bunce, J.D., *J. Am. Chem. Soc.*, 110 (1988) 5959.
- Waller, C.L., Oprea, T.I., Giolitti, A. and Marshall, G.R., *J. Med. Chem.*, 36 (1993) 4152.
- The program Sybyl 6.3 is available from Tripos Associates, St. Louis, MO.
- Weiner, S.J., Kollman, P.A., Nguyen, D.T. and Case, D.A., *J. Comput. Chem.*, 7 (1986) 230.
- Harel, M., Schalk, I., Ehret-Sabatier, L., Bouet, F., Goeldner, M., Hirth, C., Axelsen, P., Silman, I. and Sussman, J. L., *Proc. Natl. Acad. Sci. USA*, 90 (1993) 9031.
- Dougherty, D.A., *Science*, 271 (1996) 163.
- Clarc, M., Cramer III, R.D. and Van Opdenbosch, N., *J. Comput. Chem.*, 10 (1989) 982.
- Villalobos, A., Butler, T.W., Chapin, D.S., Chen, Y.L., DeMatos, S.B., Ives, J.L., Jones, S.B., Liston, D.R., Nagel, A.A., Nason, D.M., Nielsen, J.A., Ramirez, A.D., Shalaby, I.A. and Frost White, W., *J. Med. Chem.*, 38 (1995) 2802.
- Dewar, M.J.S., Zoebisch, E.G., Healy, E.F. and Stewart, J.J.P., *J. Am. Chem. Soc.*, 107 (1985) 3902.
- Cramer, R.D., Bunce, J.D., Patterson, D.E. and Frank, I.E., *Quant. Struct.-Act. Relat.*, 7 (1988) 18.
- Sussman, J.L., Harel, M., Frolow, F., Oefner, C., Goldman, A., Toker, L. and Silman, I., *Science*, 253 (1991) 872.
- Ordentlich, A., Barak, D., Kronman, Ch., Flashner, Y., Leitner, M., Segal, Y., Ariel, N., Cohen, S., Velan, B. and Shafferman, A., *J. Biol. Chem.*, 268 (1993) 17083.
- Radic, Z., Pickering, N.A., Vellom, D.C., Camp, Sh. and Taylor, P., *Biochemistry*, 32 (1993) 12074.
- Ishihara, Y., Kato, K. and Goto, G., *Chem. Pharm. Bull.*, 39 (1991) 3225.
- Fink, D.M., Bores, G.M., Effland, R.C., Huger, F.P., Kurys, B.E., Rush, D.K. and Selk, D.E., *J. Med. Chem.*, 38 (1995) 3645.
- Clementi, S. and Wold, S., In Van de Waterbeemd, H. (Ed.) *Chemometric Methods in Drug Design*, VCH, Weinheim, 1995, pp. 49–62.